Van der Waals interlayer potential of graphitic structures: From Lennard–Jones to Kolmogorov–Crespy and Lebedeva models

Zbigniew Kozioł[1,†],   Grzegorz Gawlik[2],   and   Jacek Jagielski[1,2]

[1] *National Center for Nuclear Research, Materials Research Laboratory, ul. Andrzeja Sołtana 7, 05-400 Otwock-wierk, Poland*

[2] *Institute of Electronic Materials Technology, ul. Wólczyńska 133, 01-919 Warszawa, Poland*

The experimental knowledge on interlayer potential of graphitic materials is summarized and compared with the computational results based on phenomenological models. Besides Lennard–Jones approximation, the Mie potential is discussed, as well as the Kolmogorov–Crespy model and equation of Lebedeva *et al.* An agreement is found between a set of reported physical properties of graphite (layer binding energies, compressibility along *c*-axis in a broad pressure range, Raman frequencies for bulk shear and breathing modes under pressure), when a proper choice of model parameters is taken. It is argued that anisotropic potentials, Kolmogorov–Crespy and Lebedeva, are preferable for modeling, as they provide a better, self-consistent description. A method of fast numerical modeling, convenient for the accurate estimation of the discussed physical properties, is proposed. It may be useful in studies of other van der Waals homo/heterostructures as well.

1. Introduction

There is recently a growing interest in artificial heterostructures formed by 2-dimensional (2D) layers of graphene and other newly discovered materials, and named van der Waals heterostructures.[1] This is due to richness of physical phenomena observed and high potential of their possible applications.[2] Moiré patterns result when two layers are rotated[3,4] and are related to the formation of van Hove singularities in the density of electronic states. In the bilayer graphene twisted at about $1.06°$, an unconventional superconductivity was found with a critical temperature of 1.7 K.[5–8] By manipulating the doping levels, the van Hove singularities were observed at angles up to $31°$.[9] It was shown that free-standing vdW heterostructure of graphene on hexagonal boron nitride (h-BN), where a small lattice mismatch exists, shows a buckled atomic structure formed as Moiré pattern.[10] There is already a number of laboratory prototypes of optoelectronic devices,[11] like bolometers[12] and photodetectors.[13,14] Their characteristics can be tuned by elemental doping, surface chemical doping, intercalation, electrostatic gating, strain[15] and by twisting the layers.[16]

It is believed that artificial vdW heterostructures offer a broad field for research on novel materials, such as graphene/silicene, graphene/MoS_2, and silicene/MoS_2 systems,[2] as well as silicene[17] or MoS_2 alone.[18] *Ab-initio* calculations suggest the existence of magnetism in ReS_2 doped with Co, Fe, and Ni.[19] The formation of quantum-well type-I heterostructure in van der Waals interacting monolay-ers of MoS_2 and ReS_2 has been demonstrated[20] and type-II band alignment was found in vdW heterojunction diodes based on InSe, GaS, and graphene.[21] WSe_2 and MoS_2 monolayers have been shown useful to create charge density modulation in electronic band valleys, resulting in valley polarization. Na-doped WS_2 under strain was considered as a candidate for spintronics.[22] After spin injection from a ferromagnetic electrode, the transport of spin-polarized holes within the WSe_2 layer was observed.[23] The h-BN and graphene vdW heterojunctions showed large potential of use in spintronics.[24] Light-induced negative differential transconductance phenomenon was realized on the graphene/WSe_2 heterojunction transistor.[25] Density functional theory (DFT) calculations show that vdW interactions dominate between antimonene and graphene layers and by applying an electric field between them, one can tune the height and type of the Schottky contacts.[26] Lattice dynamical theory and *ab-initio* calculations indicate the existence of piezoelectricity in 2D lattices comprising h-BN, $2H$-MoS_2, and other transition-metal dichalcogenides.[27]

It is generally thought that van der Waals interaction, ubiquitous in nature, is caused by temporal fluctuations of electronic charge that induces dipoles of random amplitude.[28] It plays a role in friction and adhesion between materials, and in absorption of molecules on surfaces. These relatively weak forces are responsible for binding between separate sheets of graphene.

While many electronic properties of graphene-based sys-

---

http://iopscience.iop.org/cpb   http://cpb.iphy.ac.cn

tems are known,[29] still there are open questions concerning the detailed form and physical mechanisms leading to the inter-plane potential in these compounds. There are two types of approaches used to describe the van der Waals potentials of graphitic systems: the *ab-initio* one based on density functional theory and the other one based on the use of empirical potentials.[30]

The DFT calculations often give underestimated values of binding energy in case of vdW interactions [31–35] and the energy difference between bindings of (preferred) AB and AA types of stacking, E_{AB} and E_{AA}, seems too large. Recent diffusion quantum Monte Carlo calculations predict for instance E_{AA}/E_{AB} of about 0.65.[36] The results however depend strongly on the functionals used to model the vdW forces.[37,38]

In this work, we compare how well several properties of graphene/graphite can be described by using a few empirical potentials. Some of them are well based on DFT calculations. An advantage of using empirical potentials relies on ease of their implementation in numerical methods. We describe a scheme of computing several basic properties based on a simple analytical approach. The method may be easily extended to the investigation of vdW homo- and heterostructures other than graphene/graphite. We demonstrate that by careful choosing the parameters of the phenomenological potentials, we may reproduce self-consistently experimental values of several physical quantities at the same time: layer binding energy, compressibility, Raman shifts observed in shear and layer breathing modes under pressure. By using our procedure, we are able to determine well how the potential interaction of atoms changes with distance between them. Knowing that is important in modeling of a range of mechanical and electronic phenomena as well.

1.1. Lennard–Jones and Mie potentials

An often used approximation of vdW potential is the 12–6 Lennard–Jones one (LJ),

$$U(r) = 4\varepsilon \left((\sigma/r)^{12} - (\sigma/r)^6 \right),$$

with only two adjustable parameters ε and σ, where r is the distance between atoms.

It reproduces well the interlayer distance and elastic constant of graphite at zero pressure. It was proved useful in describing several basic properties of C_{60} molecules[39] with $\varepsilon = 2.964$ meV and $\sigma = 3.407$ Å. It was used for modeling carbon nanotubes[40] with $\varepsilon = 4.656$ meV and $\sigma = 3.825$ Å. He *et al.*[41] used it to obtain an analytical approximation for vdW forces acting between nanotubes. Kitipornchai *et al.* extended their continuum model[42] to study vibrations of multilayered graphene sheets. It is a convenient approximation in modeling reinforcement of composite materials with carbon nanotubes.[43]

A more general form of vdW potential is the one introduced by Mie.[44,45] It often reproduces well the properties of carbon compounds: $U(r) = \alpha\varepsilon \left((\sigma/r)^m - (\sigma/r)^n \right)$, where $\alpha = (m/(m-n)) \cdot (m/n)^{n/(m-n)}$. When $m = 12$ and $n = 6$, the form of Lennard–Jones potential is assumed with $\alpha = 4$.

1.2. Kolmogorov–Crespi and Lebedeva potentials

There are two deficiencies of LJ or Mie type of potentials. The first one is that they are isotropic, i.e., the potential depends only on the distance between atoms. However, in graphitic materials, the binding between atoms on different planes is due to overlap between π orbitals from adjacent layers, as such it ought to depend on the angle between them. The second problem, as it was noticed first by Kolmogorov and Crespi (KC),[46,47] is that these potentials produce too small energy difference between bindings of AB (preferred) and AA types of stacking, E_{AB} and E_{AA}. Albeit there is some disagreement in literature regarding how large that energy difference is. The KC potential has an r^{-6} two-body van der Waals-like attraction and an exponentially decaying repulsion term, very short ranged, falling essentially to zero at two transverse interatomic distances. The directionality of the overlap is reflected by a function which rapidly decays with the transverse distance ρ. Most often it is used in the following form for interaction between atoms m and l on neighboring layers of graphene:

$$\begin{aligned} U_{lm} = &-A \left(\frac{z_0}{r_{lm}} \right)^6 + \exp\left(-\lambda\left(r_{lm} - z_0\right)\right) \\ &\times \left[C + f(\rho_{lm}) + f(\rho_{ml}) \right], \end{aligned} \tag{1}$$

with

$$f(\rho_{lm}) = \exp\left(-(\rho_{lm}/\delta)^2\right) \cdot \sum_{n=0}^{2} C_{2n} \left(\rho_{lm}/\delta\right)^{2n}, \tag{2}$$

where $\rho_{lm}^2 = r_{lm}^2 - (\boldsymbol{n}_l \cdot \boldsymbol{r}_{lm})^2$, $\rho_{ml}^2 = r_{lm}^2 - (\boldsymbol{n}_m \cdot \boldsymbol{r}_{lm})^2$, $\boldsymbol{n}_k$ is the vector normal to the sp^2 plane in the vicinity of atom k, and z_0 has a value close to the interlayer distance at equilibrium. The summation over n in Eq. (2) is usually limited from $n = 0$ to $n = 2$.

The KC potential has been used broadly in numerical modeling (molecular dynamics)[3,4,49,50] as well in description of ballistic nanofriction.[51,52]

Lebedeva *et al.*,[53,54] used another analytic function of anisotropic potential which was obtained by approximating the results of DFT calculations and was found to describe well the experimental graphite compressibility and the corrugation against sliding, while Jiang[55] used the following function for modeling the thermal conductivity of FLG:

$$\begin{aligned} U = &-A \left(\frac{z_0}{r} \right)^6 + B \exp\left(-\alpha(r - z_0)\right) \\ &+ C \left(1 + D_1 \rho^2 + D_2 \rho^4\right) \exp\left(-\lambda_1 \rho^2\right) \end{aligned}$$

$$\times \exp\left(-\lambda_2\left(z^2 - z_0^2\right)\right), \qquad (3)$$

where r is the interatomic distance, z is the interplane distance, and $\rho = \sqrt{r^2 - z^2}$ is the projection of the distance within the graphene plane.

2. Analytical approximation

Lattice spacing in graphite in hexagonal c-direction is known well from x-ray diffraction, it is 3.3538 Å at room temperature, and it does not change strongly with temperature.[56] The equilibrium interlayer spacing is 3.34 Å in AB stacked graphene[56] and 3.44 Å in turbostratic graphene.[57] Neutron diffraction studies show that all in-plane C–C lengths are 1.422 ± 0.001 Å.[58]

2.1. Distances between atoms in AB and AA stackings

There are two types of ordering of atoms on the nearest plane with respect to atoms on one plane. We will call them type I and type II orderings. The type I results when the atom is placed over another atom of the hexagon and type II is found when the atom is placed over the center of hexagon. Type I ordering is the only one present in case of AA stacking, and in case of AB (Bernal) stacking, equal numbers of atoms are in orderings of type I and type II.

We observe that atoms of both types of ordering can be grouped in rings as shown in Fig. 1, where rings of equidistant atoms are of different colors.
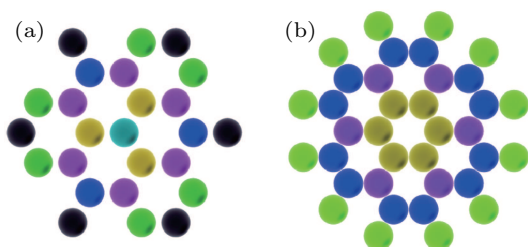

Fig. 1. Rings of equidistant atoms on neighboring planes of graphene: (a) type I ordering, present for AA and AB stacking and (b) type II ordering, present in AB stacking only.

Our aim is to find out radii of these rings and the number of atoms in any ring.

We can create a convenient scheme of calculating numerically the potential energy for different stackings by computing it for each of these types of orderings. For that, we need distances projection (in plane) between an atom position over the plane together with the number of atoms at these distances (rings of equidistant atoms, as these in Fig. 1).

2.1.1. Radius of rings of equidistant atoms

Positions of carbon atoms in a graphene lattice may be generated with the following equation:

$$(x, y) = \left(m + n/2, \sqrt{3} \cdot n/2\right), \qquad (4)$$

for pairs of integer numbers (m, n) not fulfilling the following condition: $(n \bmod 3 = 0)$ & $(m \bmod 3 = 1)$, or $(n \bmod 3 = 1)$ & $(m \bmod 3 = 2)$, or $(n \bmod 3 = 2)$ & $(m \bmod 3 = 0)$.

Accordingly, the plane projections of distances from an atom located at $(x, y) = (0, 0)$ are given by

$$\rho = \sqrt{(m + n/2)^2 + (\sqrt{3} \cdot n/2)^2} = \sqrt{m^2 + mn + n^2},$$

where the pairs of coordinates (x, y) and distances are in units of lattice parameter $a = 1.42$ Å.

2.1.2. Number of atoms in rings of equidistant atoms

We do not know how to find out the number of atoms in any ring of equidistant atoms by using an analytical formula. These numbers can however be found numerically in a few ways by using a proper algorithm, as will be described in a separate publication. The results are shown in Table 1, where ρ is the plane projection of distance, N is a pair of number of equidistant neighbors (in regular font for type I and in bold font for type II ordering). In case of type II ordering, there are always 2 times more neighbors than those for type I or none (marked by dash). Pairs (m, n) are example numbers that must be used in Eq. (4) to compute the distance accurately. Table 1 lists one only pair of (m, n), there are however more pairs of (m, n) that result in the same distances ρ.

Table 1. In-plane projection of distances between an atom on one graphene plane and the nearest neighbors on the next plane for type I of neighbors, as in Fig. 1(a), found in AA and AB stackings of layers, and for type II ordering, as in Fig. 1(b). N is a pair of number of equidistant neighbors (in regular font for type I and in bold font for type II ordering). ρ is in units of graphene unit cell value of 1.42 Å. Pairs (m, n) are example numbers that are used in Eq. (4).

m,n	0,0	0,1	1,1	2,0	1,2	3,0	2,2	3,1	0,4	2,3	1,4	5,0	3,3	4,2
ρ	0	1	1.732	2	2.645	3	3.464	3.605	4	4.358	4.582	5	5.196	5.291
N	1 –	3 **6**	6 –	3 **6**	6 **12**	6 –	6 –	6 **12**	3 **6**	6 **12**	12 –	3 **6**	6 –	6 **12**
m,n	1,5	0,6	3,4	2,5	6,1	4,4	0,7	2,6	1,7	4,5	3,6	8,0	7,2	1,8
ρ	5.567	6	6.082	6.245	6.557	6.928	7	7.211	7.549	7.810	7.937	8	8.185	8.544
N	6 **12**	6 –	6 **12**	12 –	6 **12**	6 –	9 **18**	6 **12**	12 –	6 **12**	12 –	3 **6**	6 **12**	6 **12**
m,n	5,5	6,6	3,7	0,9	2,8	9,1	4,7	8,3	0,10	2,9	6,6	7,7	1,10	4,8
ρ	8.660	8.717	8.888	9	9.165	9.539	9.643	9.848	10	10.148	10.392	10.440	10.535	10.583
N	6 –	6 **12**	6 **12**	6 –	12 –	12 **24**	12 –	6 **12**	3 **6**	6 **12**	6 –	6 **12**	12 –	6 **12**

In the numerical simulations, e.g., performed in LAMMPS,[59] it is a standard procedure to introduce a cut-off distance in equations on potential energy assuming it equal to zero when the distance between particles exceeds that value, while the function given by these equations is appropriately smoothed out in order to avoid possible discontinuities in computational results. That cut-off is taken usually at around 12 Å in case of graphene modeling. Limiting any approximation to atoms listed in Table 1 is equivalent to using a cut-off distance of about 15.4 Å.

2.1.3. Potential energy of atoms

Potential energy $\Phi_{\mathrm{I}}(z)$ for an atom in position AA at a distance z from the plane is given by an infinite sum of contributions from equidistant atoms of type I

$$\Phi_{\mathrm{I}}(z) = \sum_{i=1}^{\infty} N(i) \cdot U\left(\sqrt{(z^2 + (a \cdot \rho_i)^2)}\right), \qquad (5)$$

where the number of neighbors $N(i)$ at distance $\rho(i)$ is taken from entries of Table 1 and U is any of potentials discussed (LJ, Mie, KC, or Lebedeva's). In Eq. (5), a is the unit cell length for in-plane atoms ($a = 1.42$ Å in case of graphene).

In case of AB planes, there is equal number of atoms that are in orderings of type I and type II. The equation on energy for type II atoms, $\Phi_{\mathrm{II}}(z)$, is similar to that in Eq. (5), with summation taken on the data in Table 1 for type II atoms. We must take an average of $\Phi_{\mathrm{I}}(z)$ and $\Phi_{\mathrm{II}}(z)$ as an average energy of each atom in case of AB ordering.

Figure 2 illustrates the quick convergence of potential energy Φ as a function of the total number of atoms N in a symmetric "molecule" for type I and type II molecules computed for the LJ potential. An approximately $1/N^2$ scaling (or $1/R$, where R is the molecule radius) is obtained, when the rings of equidistant neighbors are added in Eq. (5).
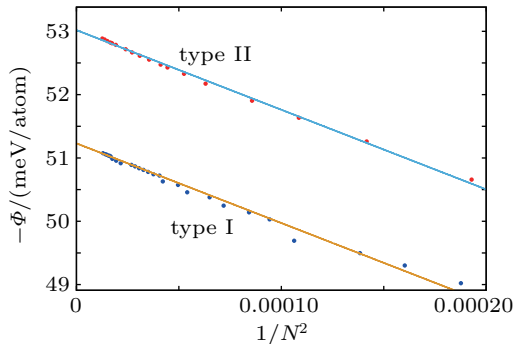
Fig. 2. Scaling of potential energy depth as a function of $1/N^2$, the number of atoms in a symmetric "molecule" for type I and II molecules, computed for the LJ potential with parameters $\varepsilon = 2.80$ meV and $\sigma = 3.38$ Å. Asymptotic splitting for $N \to \infty$ between type I and type II energy minima, $(\Phi_{\mathrm{II}} - \Phi_{\mathrm{I}})/\Phi_{\mathrm{II}}$, is 0.034. Potential of type I is related to potential in AA stacking, while potential in AB stacking is an average of potentials of type I and type II.

Hence, an average potential energy for an atom at distance z from the surface of bulk graphite is given as a sum; for

AA, AB, and ABC stackings, it is respectively

$$E_{\mathrm{AA}}(z) = \sum_{i=1}^{\infty} \Phi_{\mathrm{I}}(z + ic), \qquad (6)$$

$$E_{\mathrm{AB}}(z) = \sum_{i=1}^{\infty} \frac{1}{2}\left(\Phi_{\mathrm{I}}(z + (2i-1)c) + \Phi_{\mathrm{II}}(z + (2i-1)c)\right)$$

$$+ \sum_{i=1}^{\infty} \Phi_{\mathrm{I}}(z + 2ic), \qquad (7)$$

$$E_{\mathrm{ABC}}(z) = \frac{1}{2}\sum_{i=1}^{\infty}\left[\Phi_{\mathrm{I}}(z + 3ic) + \Phi_{\mathrm{II}}(z + 3ic)\right]$$

$$+ \left[\Phi_{\mathrm{I}}(x + (3i-1)c) + \Phi_{\mathrm{II}}(x + (3i-1)c)\right]$$

$$+ \left[\Phi_{\mathrm{I}}(z + (3i-2)c) + \Phi_{\mathrm{II}}(z + (3i-2)c)\right], \quad (8)$$

where index i enumerates the planes. In our numerical computation, we limit their number to 4, since the contribution to the potential energy from the next planes diminishes quickly: it is of the order of 90%, 10%, 2%, and 0.5% for the first, second, third, and forth planes, respectively (Fig. 3). Considering 4 planes only is equivalent to assuming a cut-off distance of $5c$, that is 16.7 Å.
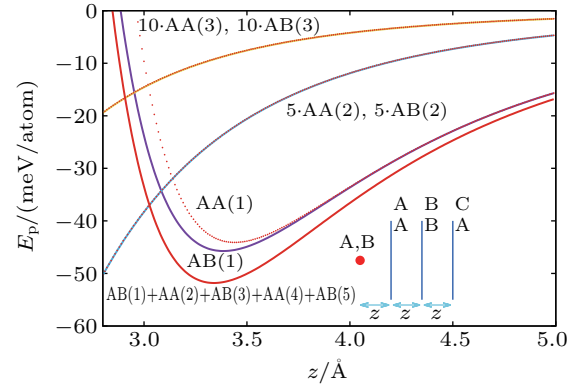
Fig. 3. Contribution to the potential energy of a single atom (represented by large red dot in the insert) as a function of distance z from the surface of three neighboring planes, separated also by distance z. The case of ABA and ABC ordering of planes is considered. The atom is considered in two positions with respect to the first plane, AA(1) or AB(1). The energy contribution from the third plane is exactly the same regardless whether it is the A plane or C plane. Energy from the second and third planes is rescaled 5 and 10 times, respectively. Classical L–J potential 12–6 with parameters $\varepsilon = 2.80$ meV and $\sigma = 3.38$ Å is used. The depth of the potential well for the lowest curve denoted as $\mathrm{AB}(1) + \mathrm{AA}(2) + \mathrm{AB}(3) + \mathrm{AA}(4) + \mathrm{AB}(5)$ (which shows the sum of energies from 5 consecutive planes in AB configuration) is 52 meV.

The proposed method of computing interlayer potential is convenient for quick testing of potentials other than those of Mie or Lennard–Jones, since this requires only replacement of the function $U(z)$ in Eq. (5) by another one.

In case of perfect AA or AB stacking, due to the symmetry, the π-orbitals must point out in directions normal to the planes. In this case, in Kolmogorov–Crespi equations (1) and (2), the values of $n_l \cdot r$ and $n_m \cdot r$ reduce to z, where z is the distance of an atom from the plane. That is, ρ_{lm} and ρ_{ml} become equal to ρ from Table 1. We may rewrite Eqs. (1) and

(2) in the form

$$U_{\text{KC}} = -A\left(\frac{z_0}{r}\right)^6 + \exp\left(-\lambda\left(r - z_0\right)\right)$$

$$\times \left[C + 2\exp\left(-(\rho/\delta)^2\right) \cdot \sum_{n=0}^{2} C_{2n}\left(\rho/\delta\right)^{2n}\right]. \quad (9)$$

where $r = \sqrt{z^2 + \rho^2}$. Similarly, we may rewrite Lebedeva's version of potential as

$$U_{\text{Leb}} = -A\left(\frac{z_0}{r}\right)^6 + B\exp\left(-\alpha\left(r - z_0\right)\right)$$

$$+ C\left(1 + D_1\rho^2 + D_2\rho^4\right)$$

$$\times \exp\left(-\lambda_1\rho^2\right)\exp\left(-\lambda_2\left(z^2 - z_0^2\right)\right). \quad (10)$$

In case of Lennard–Jones potential, the results presented here are computed with $\varepsilon = 2.4$ meV and $\sigma = 3.4322$ Å. For the models of Kolmogorov–Crespi and Lebedeva *et al.*, we used values of parameters listed in Tables 2 and 3, respectively (LAMMPS implementation of equation of Lebedeva *et al.* is now available from GitHub repository of LAMMPS or from the corresponding author). One ought to be aware that usually there is a broad range of parameters values for any of the above models of potential that may provide functionally nearly identical dependencies $U(z)$ and reasonable agreement with experiments; compare for instance Refs. [47] and [52] with Refs. [46] and [50]. The original parameters of Lebedeva equation were derived by fitting to results of *ab-initio* DFT modeling and with the purpose of describing graphene corrugation experiments. The values of the parameters used by us allow for a reasonably good fitting of several physical properties of graphene at the same time.

Table 2. Summary of parameters' values used in Kolmogorov–Crespi equation (9).

A/meV	C/meV	C_0/meV	C_2/meV	C_4/meV	z_0/Å^{-1}	λ/Å^{-1}	δ/Å	Ref.
10.238	3.030	15.71	12.29	4.933	3.34	3.629	0.578	[47], [52]
9.89	0.7	5.255	2.336	1.168	3.449	3.2	2.1	this work, set A
8.881	0.6286	4.719	2.098	1.049	3.487	3.4	1.7	this work, set B

Table 3. Summary of parameters' values used in Lebedeva equation (10).

A/meV	B/meV	C/meV	α/Å^{-1}	z_0/Å	λ_1/Å^{-2}	λ_2/Å^{-2}	D_1/Å^{-2}	D_2/Å^{-4}	Ref.
10.510	11.652	35.883	4.16	3.34	0.48703	0.46445	−0.86232	0.10049	[53]
14.558	21.204	1.8	4.16	3.198	0.6	0.4	−0.862	0.10049	this work

3. Computed results

3.1. Compressibility

Equation (7) may be used for computing compressibility along c-axis. Pressure acting on one atom is equal to force (which is the derivative of the potential energy over spacing between layers) divided by area per one atom (which is $3\sqrt{3}/2a^2$), $P(c) = \eta \cdot dE_{\text{AB}}(c)/dc$, where c is the lattice constant perpendicular to the planes under pressure P and $\eta = 30.54$ GPa·eV^{-1}·Å^{-3}. The first and second derivatives of $E_{\text{AB}}(z)$ could be computed by using the derived analytical expressions. Numerical approach of finding derivatives is however convenient to implement and fast.

Figure 4 shows the found ratio of c/c_0 as a function of pressure for LJ, KC, and Lebedeva potentials, with parameters as these in Tables 2 and 3. In case of LJ model, the parameter ε used was 3.3 meV, which leads to a binding energy of 64 meV/atom, larger than the most commonly accepted value of around 50 meV/atom but leading to better agreement between results of other calculations and measurements, as reported in the following sections. The straight solid line with a slope of -0.029 GPa^{-1} at $P = 0$ for the LJ potential corresponds to elasticity modulus $C_{33} = 38.5$ GPa, and for the KC one the slope gives $C_{33} = 43.5$ GPa, in a very good agreement with experiment. *Ab-initio* DFT computations gave a broader spread of values, from 43.6 GPa to 67.5 GPa.[60]

The pressure dependence of c can be found or deduced from several measurements.[58,61–63,65] The experimental results in Fig. 4 have a broad dispersion of data points, which is, in part, due to subtle differences in the used measurement techniques.
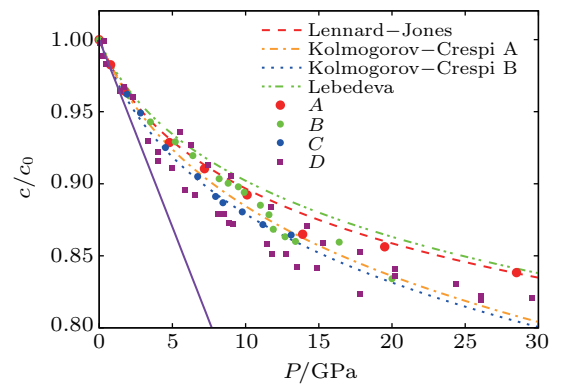

Fig. 4. Compressibility of graphite along c-axis. The curves are computed numerically by using Eq. (3) with L–J, K–C, and Lebedeva potentials. The straight solid line fits the slope at $P = 0$ of data computed for the KC potential, which corresponds to elasticity modulus $C_{33} = 43.5$ GPa. Data points are collected from works of Lynch and Drickamer (Ref. [62], *A*), Zhao and Spain (Ref. [63], *B*), Hanfland *et al.* (Ref. [64], *C*), and Clark *et al.* (Ref. [65], *D*).

3.2. Stacking order

There is much controversy around prevailing stacking order in graphite and in a few layers graphene (FLG). It is known that there are three types of stacking, an AA one, which is simple hexagonal (it is not found in natural graphite and exists only in intercalated compounds such as C_6Li and C_8K), an AB stacking, hexagonal, known also as Bernal, and a rhombohedral ABC stacking. Additionally, a random stacking of these three types is called a turbostratic TS structure and often is obtained in laboratories. In bulk graphite, it was reported that the volume fraction AB : ABC : TS was about 80 : 14 : 6.[74]

Lee et al.[66] were able to obtain AA structured graphene on diamond surface, with an interplanar spacing of ~ 3.55 Å. The value is between those of the AB graphite (3.35 Å) and the lithium intercalated AA graphite 3.706 Å.[67] Norimatsu and Kusunoki[68] observed ABC-stacked graphene on the SiC substrate and interpreted their results in terms of possible modification of second-plane interactions by the substrate, as explained by the Slonczewski–Weiss–McClure model.[69] Yoshizawa et al.[70] proposed that the AB stacking of layers in graphite is a consequence of orbital interactions between layers rather than that of generally accepted van der Waals forces.

The energy difference between AA and AB was reported to be 17.31 meV/atom,[36] in favor of AB, while between ABC and AB it was reported as 0.11 meV/atom,[71] which are both based however on DFT calculations only.

It was observed that in the case of graphene, its bilayer exhibits AB stacking while trilayer prefers ABC stacking.[72] When the number of layers increases, again AB stacking is favored. The binding energies are found to increase from 23 meV/atom in bilayer to 39 meV/atom in pentalayer, while the interlayer distance decreases from 3.37 Å in bilayer to 3.35 Å in pentalayer. Our models do not reproduce so strong change of binding energy with number of layers. In 2-layer graphene, we find around 90% of binding energy per atom of that in bulk graphite when the LJ model is used (Fig. 4). However, the change of interlayer distance agrees with that reported[73] for all three models discussed.

If we assume that the interaction between next nearest planes (NNP) is negligible, then there is no reason for difference in stability of ABC and AB structures. Hence the NNP interaction must play a role.

The explanation to the AB : ABC ratio observed of about 80 : 14[74] could be found by adding to already existing isotropic attractive term of vdW potential a small anisotropic contribution to equations like those of KC or Lebedeva. Since interplane binding is caused by the strongly anisotropic interaction between π orbitals, one would expect that not only repulsive but also attractive component of that interaction is anisotropic.

3.3. Raman shifts in breathing and shear modes (C_{33} and C_{44} elastic constants)

Early neutron scattering measurements confirmed the existence of the low-frequency acoustic mode in bulk pyrolitic graphite,[75] that is, the longitudinal waves in the direction of the hexagonal axis, at 3.84 ± 0.06 THz. The transverse waves (in shear mode) were less pronounced, at 1.3 ± 0.3 THz. Based on these data, the elastic constants have being deduced, $C_{33} = 39 \pm 4$ GPa (for direction perpendicular to the graphite planes) and $C_{44} = 4.2 \pm 2$ GPa (shear mode parallel to the planes). These values correspond to Raman shift energies of 130 cm^{-1} and 43 cm^{-1}, in agreement with several DFT calculations.[76] The experimental evidence of the longitudinal mode was reported in ultrafast laser pump–probe spectroscopy[77] on FLG at ~ 120 cm^{-1}, demonstrating also the presence of the phonon and electron coupling there through the Breit–Wigner–Fano resonance, as at more pronounced G-mode.[78]

Position of peaks in both breathing and shear modes is a geometrical effect and it depends strongly on the number of layers in FLG. Moreover, unique multipeak features are observed, characteristic for the number of layers investigated. Their frequencies in case of breathing mode[79] are described well using a simple linear-chain model based on nearest-neighbor couplings between the layers,[80] $\omega_N(n) = \omega_0 \sin[(N-n)\pi/2N]$, where ω_0 is the frequency of the bulk mode, N is the number of layers in FLG, and n enumerates the observed Raman frequencies.

For the shear mode, the nature of interactions between planes, their collective behavior, leads to quantitatively similar dependence of Raman frequencies on the number of layers in FLG as in the case of breathing mode: the frequency in the bulk is $\sqrt{2}$ times larger than that for bilayer graphene.[81,82] That frequency depends mainly on the energy difference between AB and AA stackings. For this reason, modeling it is sensitive to the choice of the inter-plane interaction potential.

In Fig. 5, we show how the potential energy changes when a graphene plane lying over another graphene plane moves away from the AB position by 1.42 Å towards AA stacking. These calculations were made in LAMMPS, assuming LJ potential with $\sigma = 3.4322$ Å and $\varepsilon = 2.4$ meV. We find that the energy difference between planes in AA and AB positions is of around 1 meV/atom only at $P = 0$ GPa.

By having the curvature of the parabolic potential wells at low-values of departure from the optimal position of both layers (i.e., from AB stacking position; we used data for x less then 0.05 Å), we are able to compute Raman frequencies in shear mode in a broad range of pressure. The curvature k of the parabolic fit of data in Fig. 5, $E_p(x) - E_{AB} = k/2 \cdot x^2$, leads to vibration frequency f in classical oscillator equation: $f = 1/2\pi \sqrt{k/m}$, where m is the mass of one atom of carbon. We may write that as $R[\text{cm}^{-1}] = \sqrt{2} \cdot \sqrt{k} \cdot 150.467$, where R

is the Raman shift and k is in units of eV/Å^2. The $\sqrt{2}$ factor is to account that the bulk potential acting on a plane is twice as large as the potential for a single plane on the surface of a rigid sample.
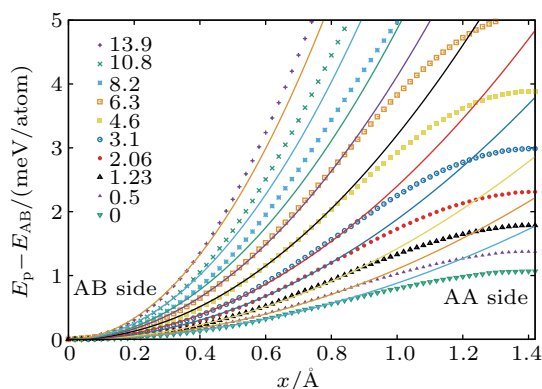

Fig. 5. Data points show change in potential energy of a plane that is moved from AB position over another large plane by a distance of $a = 1.42$ Å, which results in AA position, under several values of pressure [GPa] as listed in the legend. The classical 12–6 Lennard–Jones potential was used in modeling, with $\sigma = 3.4322$ Å and $\varepsilon = 2.4$ meV. Solid lines show a tentative fit of the parabolic dependencies.

The results on Raman shift are shown in Fig. 6, where a comparison is made of the data obtained by using LJ, Lebedeva, and KC potential models (for KC with two sets of parameters), as listed in Tables 2 and 3. The data in Fig. 6 are compared with the experimental results of Hanfland *et al.*[64] It is evident that the LJ potential can not describe well the measured values of Raman shift, as it is about twice too low at $P = 0$ GPa with that observed in experiment. Both KC and Lebedeva models allow to achieve an acceptable fit to the real data.
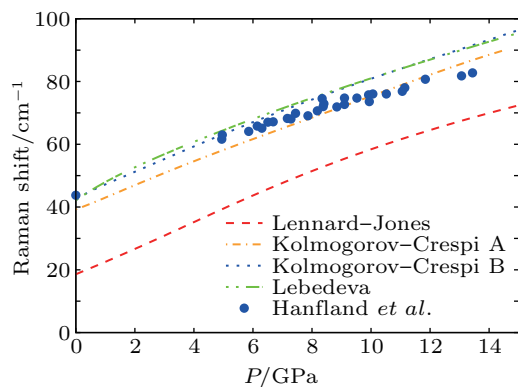

Fig. 6. Raman shift energy as a function of pressure for bulk shear mode. The lines are computed from curvature k of parabolic fit of data in Fig. 5. Blue circles are the experimental data of Hanfland *et al.*[64]

For the breathing mode, the results on Raman shift are only known at $P = 0$ GPa and our calculations reproduce that value well.[79] The scheme described in this section offers a convenient way of numerical computing the frequency of oscillations as a function of pressure, by starting with Eq. (7). One needs for that to use also the data available in Fig. 4 and

find out from there how planes' spacing c changes with pressure. We insert c values into Eq. (7) and numerically find out the second derivative $\mathrm{d}^2E_{AB}(z)/\mathrm{d}z^2$, which gives us the curvature of potential at the potential minima and next the frequencies of Raman shift as a function of pressure. The results are shown in Fig. 7, computed for the LJ, KC, and Lebedeva models. If similar experimental data were available, we could have an additional indication on which of considered models of vdW interactions fits best to reality.
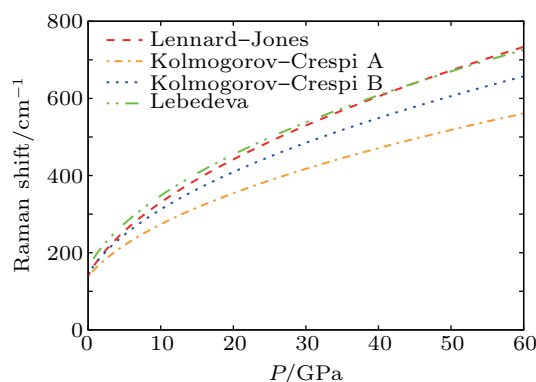

Fig. 7. Predicted pressure dependence of Raman shift for breathing mode of bulk graphite.

4. Conclusion

Modeling of interlayer interaction in graphitic materials was performed based on phenomenological van der Waals potentials (Lennard–Jones, Kolmogorov–Crespi, and Lebedeva's). The results have been compared self-consistently with existing *ab-initio* calculations and experimental data on compressibility and Raman shifts in breathing and shear modes under pressure, favoring strongly the anisotropic models of potential. Computation was done by using molecular dynamics package LAMMPS and a proposed convenient, extendable scheme suitable for fast numerical modeling of several physical quantities. The method is useful for studying other 2-dimensional homo- and heterostructures with van der Waals type interaction between layers. In case of homostructures, the application of the proposed method is straightforward. In case of twisted homostructures or heterostructures, such as h-BN/graphene, some approximations would need to be introduced due to the lattice mismatch between components. The proposed method could possibly be extended to studies of other lattices, different than hexagonal and to other physical phenomena where interactions decaying quickly with distance are involved.

References

[1] Geim A K and Grigorieva I V 2013 *Nature* **499** 419
[2] Le N B, Huan T D and Woods L M 2016 *ACS Appl. Mater. Interfaces* **9** 6286
[3] Wijk M M V, Schuring A, Katsnelson M I and Fasolino A 2015 *2D Materials* **2** 34010

[4] Wijk M M V, Schuring A, Katsnelson M I and Fasolino A 2014 *Phys. Rev. Lett.* **113** 135504

[5] Cao Y, Fatemi V, Fang S, Watanabe K, Taniguchi T, Kaxiras E and Jarillo-Herrero P 2018 *Nature* **43** 556

[6] Bistritzer R and MacDonald A H 2011 *Proc. Nat. Acad. Sci.* **108** 12233

[7] Tarnopolsky G, Kruchkov A J Vishwanath A 2019 *Phys. Rev. Lett* **122** 106405

[8] Cao Y, Fatemi V, Fang S, Watanabe K, Taniguchi T, Kaxiras E and Jarillo-Herrero P 2018 *Nature* **556** 43

[9] Peng H, Schröter N B M, Yin J, Wang H, Chung T F, Yang H, Ekahana S, Liu Z, Jiang J, Yang L, Zhang T, Ni H H, Barinov A, Chen Y P, Liu Z, Peng H and Chen Y 2017 *Adv. Mater.* **1606741**

[10] Argentero G, Mittelberger A, Monazam M R A, Cao Y, Pennycook T J, Mangler C, Kramberger C, Kotakoski J, Geim A K and Meyer A J C 2017 *Nano Lett.* **17** 1409

[11] Lin S, Lu Y, Xu J, Feng S and Li J 2017 *Nano Energy* **40** 122

[12] Skoblin G, Sun J and Yurgens A 2018 *Appl. Phys. Lett.* **112** 063501

[13] Wei X, Yan F G, Shen C, Lv Q S and Wang K Y 2017 *Chin. Phys. B* **26** 038504

[14] Congpu M, Jianyong X and Zhongyuan L 2017 *J. Mater. Res.* **32** 4115

[15] Celebonovic V, Pesic J, Gajic R, Vasic B and Matkovic A 2019 *J. Appl. Phys.* **125** 154301

[16] Wang J G, Mu X J, Sun M T and Mu T J 2019 *Appl. Mater. Today* **6** 1

[17] Houssa M, Dimoulas A and Molle A 2015 *J. Phys.: Condens. Matter* **27** 253002

[18] Kvashnin D G and Chernozatonskii L A 2017 *JETP Lett.* **105** 250

[19] Luo M, Shen Y H and Yin T L 2017 *JETP Lett.* **105** 255

[20] Bellus M Z, Li M, Lane S D, Ceballos F, Cui Q, Zeng X C and Zhao H 2017 *Nanoscale Horiz.* **2** 31

[21] Yan F, Zhao L, Patanè A, Hu P A, Wei X, Luo W, Zhang D, Lv Q, Feng Q, Shen C, Chang K, Eaves L and Wang K 2017 *Nanotechnology* **28** 27LT01

[22] Luo M, Yin H H and Chu J H 2017 *JETP Lett.* **6** 672

[23] Sanchez O L, Ovchinnikov D, Misra S, Allain A and Kis A 2016 *Nano Lett.* **16** 5792

[24] Gurram M, Omar S and Wees B J V 2017 *Nat. Commun.* **8** 248

[25] Shim J, Jo S, Kim M, Song Y J, Kim J and Park J 2017 *ACS Nano* **11** 6319

[26] Li W, Wang X and Dai X 2017 *Solid State Commun.* **254** 37

[27] Michel K H, Çakır D, Sevik C and Peeters F M 2017 *Phys. Rev. B* **95** 125415

[28] Kawai S, Foster A S, Björkman T, Nowakowska S, Björk J, Canova F F, Gade L H, Jung T A and Meyer E 2016 *Nat. Commun.* **7** 11559

[29] Rozhkov A, Sboychakov A, Rakhmanov A and Nori F 2016 *Phys. Rep.* **648** 1

[30] Girifalco L A and Hodak M 2002 *Phys. Rev. B* **65** 125404

[31] Charlier J, Gonze X and Michenaud J 1994 *Europhys. Lett.* **28** 403

[32] Trickey S B, Müller-Plathe F, Diercksen G H F and Boettger J C 1992 *Phys. Rev. B* **45** 4460

[33] Rydberg H, Dion M, Jacobson N, Schröder E, Hyldgaard P, Simak S I, Langreth D C and Lundqvist B I 2003 *Phys. Rev. Lett.* **91** 126402

[34] DiVincenzo D P, Mele E J and Holzwarth N A W 1983 *Phys. Rev. B* **27** 2458

[35] Schabel M C and Martins J L 1992 *Phys. Rev. B* **46** 7185

[36] Mostaani E, Drummond N D and Fal'ko V I 2015 *Phys. Rev. Lett.* **115** 115501

[37] Birowska M, Milowska K and Majewski J 2011 *Acta Phys. Pol. A* **120** 845

[38] Chakarova-Kack S D, Schroder E, Lundqvistand B I and Langreth D C 2006 *Phys. Rev. Lett.* **96** 146107

[39] Lu J P, Li X P and Martin R M 1992 *Phys. Rev. Lett.* **68** 1551

[40] Jiang L, Huang Y, Jiang H, Ravichandran G, Hwang H G and Liu B 2006 *J. Mech. Phys. Solids* **54** 2436

[41] He X, Kitipornchai S and Liew K 2005 *J. Mech. Phys. Solids* **53** 303

[42] Kitipornchai S, He X Q and Liew K M 2005 *Phys. Rev. B* **72** 075443

[43] Tan H, Jiang L, Huang Y, Liu B and Hwang K 2007 *Compos. Sci. Technol.* **67** 2941

[44] Mie G 1903 *Ann. Phys.* **316** 657

[45] Avendano C, Lafitte T, Galindo A, Adjiman C S, Jackson G and Muller E 2011 *J. Phys. Chem. B* **115** 11154

[46] Kolmogorov A N and Crespi V H 2000 *Phys. Rev. Lett.* **85** 4727

[47] Kolmogorov A N and Crespi V H 2005 *Phys. Rev. B* **71** 235415

[48] Naik M H, Maity I, Maiti P K, and Jain M 2019 *J. Phys. Chem. C* **123** 9770

[49] Wijk M M V, Schuring A, Katsnelson M I and Fasolino A 2014 *Phys. Rev. Lett.* **113** 135504

[50] Schuring A 2014 *Master Thesis* (Radbound University Niimegen)

[51] Ng T W, Lau C Y, Bernados-Chamagne E, Liu J Z, Sheridan J and Tan N 2012 *Nanoscale Res. Lett.* **7** 185

[52] Guerra R, Tartaglino U, Vanossi A and Tosatti E 2010 *Nat. Mater.* **9** 634

[53] Lebedeva I V, Knizhnik A A, Popov A M, Lozovik Y E and Potapkin B V 2012 *Physica E* **44** 949

[54] Lebedeva I V, Knizhnik A A, Popov A M, Lozovik Y E and Potapkin B V 2011 *Phys. Rev. B* **84** 245437

[55] Jiang J 2014 *J. Appl. Phys.* **116** 164313

[56] Baskin V and Meyer L 1955 *Phys. Rev. B* **100** 544

[57] Kiang C H, Endo M, Ajayan P M, Dresselhaus G and Dresselhaus M S 1998 *Phys. Rev. Lett.* **81** 1869

[58] Trucano P and Chen R 1975 *Nature* **258** 136

[59] Plimpton S 1995 *J. Comp. Phys.* **7** 1

[60] Gao W and Huang R 2011 *J. Phys. D* **44** 452001

[61] Wang Y, Panzik J E, Kiefer B and Lee K K M 2012 *Sci. Rep.* **2** 520

[62] Lynch R W and Drickamer H G 1966 *J. Chem. Phys.* **44** 181

[63] Zhao Y X and Spain I L 1989 *Phys. Rev. B* **40** 993

[64] Hanfland M, Beister H and Syassen K 1989 *Phys. Rev. B* **39** 12598

[65] Clark S, Jeon K, Chen J and Yoo C 2013 *Solid State Commun.* **4** 15

[66] Lee J, Lee S, Ahn J, Kim S, Wilson J I B and John P 2008 *J. Chem. Phys.* **129** 234709

[67] Dahn J R, Fong R and Spoon M J 1990 *Phys. Rev. B* **42** 6424

[68] Norimatsu W and Kusunoki M 2010 *Phys. Rev. B* **81** 161410

[69] Charlier J, Gonze X and Michenaud J 1991 *Phys. Rev. B* **43** 4579

[70] Yoshizawa K, Kato T and Yamabe T 1996 *J. Chem. Phys.* **105** 2099

[71] Charlier J C, Gonze X and Michenaud J P 1994 *Carbon* **32** 289

[72] Gao W and Tkatchenko A 2015 *Phys. Rev. Lett.* **114** 096101

[73] Tao W, Qing G, Yan L and Kuang S 2012 *Chin. Phys. B* **21** 067301

[74] Lipson H and Stokes A 1942 *Proc. Roy. Soc. A* **181** 101

[75] Dolling G and Brockhouse B N 1962 *Phys. Rev.* **128** 1120

[76] Lebedev A V, Lebedeva I V, Popov A M and Knizhnik A A 2017 *Phys. Rev. B* **96** 085432

[77] Shang J, Cong C, Zhang J, Xiong Q, Gurzadyan G G and Yu T 2013 *J. Raman Spec.* **44** 70

[78] Baranowski J M, Mozdzonek M, Dabrowski P, Grodecki K, Osewski P, Kozlowski W, Kopciuszynski M, Jalochowski M and Strupinski W 2013 *Graphene* **2** 115

[79] Lui C H and Heinz T F 2013 *Phys. Rev. B* **87** 121404

[80] Thornton S T and Marion J B 2003 *Classical Dynamics of Particles and Systems* (5th edn.) (Brooks Cole, Pacific Grove, CA)

[81] Tan P H, Han W P, Zhao W J, Wu Z H, Chang K, Wang H, Wang Y F, Bonini N, Marzari N, Savini G, Lombardo A and Ferrari A C 2012 *Nat. Mater.* **11** 294

[82] Cong C and Yu T 2014 *Nat. Commun.* **5** 4709